

Electron Beam Surface Hardening of Steel C45

Abstract: Surface hardening makes it possible to obtain high wear resistance of components exposed to friction without the need for hardening the entire element, thereby reducing stresses and deformations as well as process costs. The electron beam, due to its ease of dynamic deflection and focusing as well as very high heating rates, makes it possible to obtain surface layers of required properties. The article presents results of metallographic tests and Vickers hardness tests of electron beam hardened shafts made of steel grade C45. The hardening process resulted in the obtainment of layers having thickness not exceeding 400 μm and hardness not exceeding 900 HV_{0.1}.

Keywords: hardening, surface/case hardening, electron beam, surface processing, steel, 45, C45

DOI: [10.17729/ebis.2022.6/3](https://doi.org/10.17729/ebis.2022.6/3)

Introduction

Electron beam surface hardening consists in bombarding the surface of an element with electrons. The temperature of the surface grows as a result of the transformation of the kinetic energy of accelerated electrons into thermal energy. The obtainment of the martensitic structure requires that the proportion of mass subjected to hardening to that not subjected to hardening should be sufficiently high to provide the absorption of heat ensuring the obtainment of a cooling rate higher than the critical temperature of a given material. The hardening of only the surface layer of elements decreases stresses and strains as well as reduces the consumption of energy and, consequently, the cost of fabrication [1–6].

Advantages of electron beam hardening [1–6]:

- high welding rates of up to 10^9 K/s, making it possible to heat the surface of an element faster than its heat conductivity,
- precise adjustment of process parameters,
- high process precision and repeatability,
- easy automation,
- high energy conversion efficiency (exceeding 90%),
- metallurgical purity of the process (performed in vacuum),
- precise computer-aided beam deflection and focusing control enabling the hardening of elements characterised by complicated geometry.

Disadvantages of electron beam hardening [1–6]:

mgr inż. Piotr Śliwiński, mgr inż. Kamil Kubik, Łukasiewicz – Instytut Spawalnictwa (Łukasiewicz Research Network – Institute of Welding); dr inż. Mateusz Kopyściański – Akademia Górniczo-Hutnicza (AGH University of Science and Technology)

- necessity of creating appropriate vacuum, extending process auxiliary time,
- workpiece dimensions limited by the dimensions of a vacuum working chamber,
- emission of X-radiation requiring appropriate protections (lead screens, lead sight glasses) and periodic specialist inspections,
- necessity of the demagnetisation of magnetised elements before hardening.

Overview of tests involving the hardening of steel C45

Steel C45 (1.0503), one of the most popular toughened steel grades, is characterised by very good hardenability. Because of its properties, the aforesaid steel is widely used in the production of tools and machinery elements such as shafts, spindles, toothed wheels, axles, cutters, hubs, injection moulds, rods, pump rotors, etc. [7–9]. Figure 1 presents the continuous TTT diagram for steel grade C45 (1.0503).

In tests discussed in publication [11], specimens made of steel AISI 1045 (C45) were held for 60 minutes at a temperature of 880°C and, next, subjected to hardening in the 10%, 15%, 20% and 25% aqueous solution of polyvinylpyrrolidone (PVP). Microhardness values measured after the hardening process amounted to 910 HV, 874 HV, 844 HV and 830 HV respectively. The highest microhardness was obtained after hardening in the solution

characterised by the lowest concentration of polyvinylpyrrolidone.

In tests discussed in article [12], shafts made of steel C45 and having a diameter of 20 mm were subjected to induction hardening. The use of a travel rate of 20 mm/s, a frequency of 27 kHz and a power of 31 kW enabled the obtainment of a hardening depth of a nearly 2 mm. The hardness of the elements was restricted within the range of 650 HV to 750 HV.

The use of Nd:Yag laser-based hardening (laser power being 500 W) enabled the authors of publication [13] to obtain hardness restricted within the range of 700 HV to 800 HV and a hardening depth of 1.9 mm. In tests discussed in work [14], the application of a CO₂ laser for the hardening of elements made of steel C45 enabled the obtainment of very thin hardened layers, the thickness of which did not exceed 0.2 mm. The maximum hardness of the aforesaid layers amounted to 567 HV.

Overview of electron beam surface hardening tests

Publication [15] discusses tests concerning the effect of electron beam hardening on the properties and structure of tool steel AISI D3. The tests led to the obtainment of 0.4 mm thick layers. The highest hardness of approximately 1400 HV_{0.1} was identified in a specimen processed using the highest hardening rate,

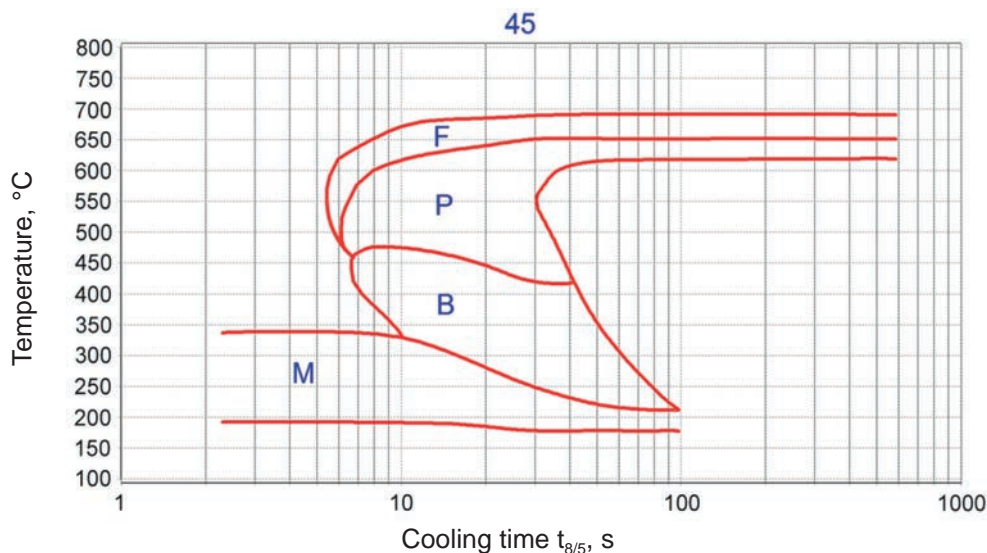


Fig. 1. Continuous TTT diagram for steel grade C45 [10]

whereas the lowest hardness amounting to less than 1000 HV_{0.1} was determined in a specimen processed using the lowest hardening rate. The hardness of the base material amounted to 650 HV_{0.1}. Each of the specimens contained an interlayer characterised by lower hardness (amounting to approximately 400 HV_{0.1}). Figure 2 presents the distribution of hardness in all of the test specimens.

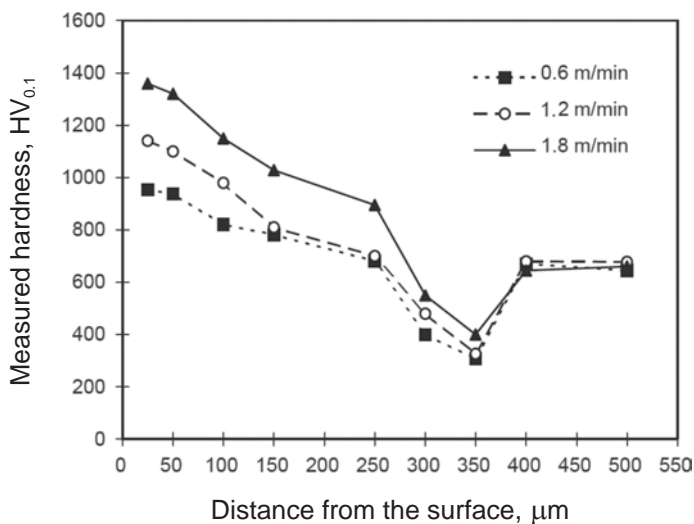


Fig. 2. Distribution of hardness in electron beam hardened specimens in relation to various hardening rates [15]

The electron beam hardening technology is also applied successfully in the automotive industry. Tests discussed in publication [16] (performed by Isuzu Motors Ltd.) were concerned with the local electron beam effect on a specimen, the effect resulting from various values of electron beam current as well as the influence of various times of electron beam effect. The material used in the tests was steel 34CrMo4. The maximum hardening depth obtained during the tests amounted to 0.9 mm. The abrasive wear resistance of an element subjected to the hardening process was by twice higher than that of an element not subjected to hardening.

The test results were satisfactory enough to take a decision to apply the electron beam hardening process in the hardening of tappets in the Isuzu B6 engine and of the contact surface of the clamping ring of the gearbox synchroniser.

Publication [17] discusses the application of the electron beam hardening process in the reconstruction of turbine blades. The restoration of the primary properties of the elements necessitated grinding off stellite layers, followed by electron beam surface hardening. After the electron beam hardening process, the surface hardness was restricted within the range of 700 HV_{0.03} to 800 HV_{0.03}, which enabled the further operation of the blades. According to the authors, the cost of the process fifteen times lower than the making of a new blade.

Article [18] discusses tests concerning the effect of various modes of electron beam oscillation on properties of hardened layers. The tests revealed that the deflection mode only slightly affected the hardness of test pieces, yet that both perpendicular and parallel deflection resulted in the growth of grains. Geometrical profiles of the cross-section of beads varied depending on applied oscillation patterns. The authors demonstrated that the hardening rate only affected the hardening depth (growing along with the decreasing hardening rate). The maximum hardness amounted to 740 HV_{0.5}. The hardening depth was restricted within the range of 0.1 mm to 1.5 mm. Figure 3 presents the effect of the beam deflection mode on the geometry of hardened layers.

The authors of publication [19], presenting results of tests concerning the optimisation of the electron beam hardening process, demonstrated that:

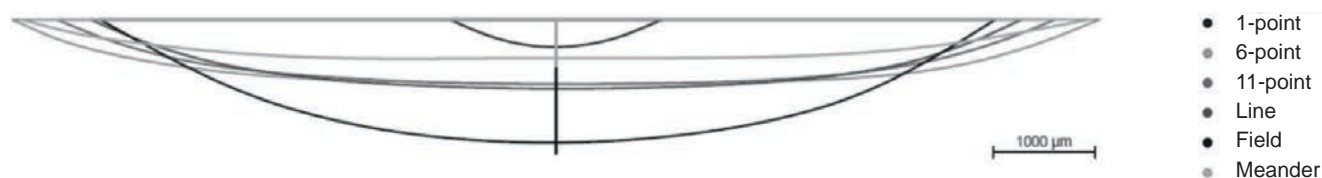


Fig. 3. Effect of the beam deflection mode on the geometry of hardened layers [18]

- heating rate grew linearly along with an increase in electron beam power, if combined with a constant specimen travel rate,
- heating rate increased along with a specimen travel rate, if combined with constant electron beam power,
- cooling rate strongly depended on the travel rate, if combined with constant electron beam power,
- cooling rate only slightly depended on electron beam power, if combined with a constant specimen travel rate.

Publication [20] also presents results of tests focused on the optimisation of the electron beam hardening process. The authors performed the mathematical simulation concerning the effect of process parameters on the microstructure and the depth of hardened layers and, next, performed technological tests involving actual elements and the oscillating electron beam. The hardening depth was restricted within the range of 0.3 mm to 1.1 mm, whereas the highest hardness amounted to 60 HRC. Based on the test results the authors demonstrated that the hardening rate and, as

a result, surface hardness, was primarily affected by the resultant electron beam power. In turn, the hardening depth depended on the density of electron beam energy on the surface of an element subjected to hardening.

The analysis of the publications concerning the hardening of steel C45 revealed that conventional hardening methods (induction hardening, in a furnace) and laser hardening methods enabled the obtainment of hardness restricted within the range of 750 HV to 910 HV. In turn, the overview of works related to electron beam hardening justified the application of the aforesaid method in surface hardening as it enabled the obtainment of layers characterised by very good properties within a wide range of thicknesses. In addition, the use of the technology enabled the hardening of elements characterised by complicated geometry such as turbine blades, tappets in combustion engines or clamping rings in gearbox synchronisers.

Testing methodology

Hardening tests performed at Łukasiewicz Research Network – Institute of Welding in

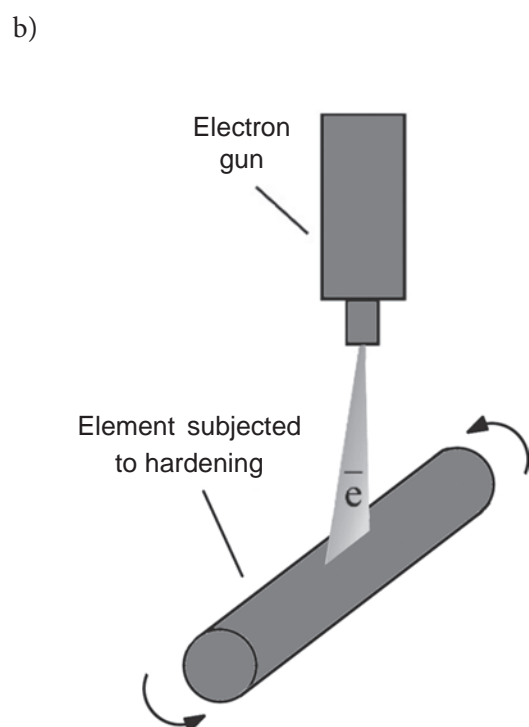


Fig. 4. View of a) shafts in the fixing clamp and b) schematic diagram of the electron beam hardening process

Gliwice involved the use of a CVE EB756 machine (model XW 150:30) having a maximum power of 30 kW and an accelerating voltage of 150 kV. Elements subjected to hardening were shafts made of steel grade C45 (1.0503), having a diameter of 17 mm and a length of 200 mm. Figure 4 presents the fixing of test specimens and the schematic diagram of the electron beam hardening process.

The tests involved the application of an accelerating voltage of 60 kV, a welding rate of 1.589 m/min (limited by the shaft diameter and the turntable rotation rate) and an electron beam current of 25 mA, 26 mA, 27 mA, 28 mA and 29 mA. The hardening process did not result in the partial melting of the surface of any of the specimens used in the tests. All the hardened beads were sampled for cross-sectional specimens, subsequently subjected to metallographic tests performed using an optical microscope (OM) or a scanning electron microscope (SEM). All of the specimens were subjected to polishing and etching in 2% Nital. The microhardness of the specimens was measured using the Vickers hardness tester and a load of 0.1 kg.

Test results

The surface hardening process led to the formation of the heat affected zone (HAZ) composed of two layers, i.e. a hardened layer and an interlayer. Figure 5 presents the cross-sectional fragment containing both HAZ layers and the base material. The first layer (dark-etched) constituted the hardened layer near the specimen surface. The light-etched layer (located below) constituted the interlayer. The layer below the HAZ area was the unprocessed base material.

In the as-received state, the microstructure of the test steel contained pearlite and ferrite (see Figure 6a). Figure 6b presents the martensitic microstructure of the hardened surface layer of the specimen subjected to hardening performed using an electron beam power of 29 mA.

As can be seen in Figure 7, the microstructure of the interlayer was the mixture of ferrite, pearlite and martensite (formed as a result of transformation taking place in the areas rich in pearlite).

Table 1 presents tests results concerning the HAZ depth along with the maximum hardness (in relation to each specimen). Figures 8 through 10 present hardness in the function

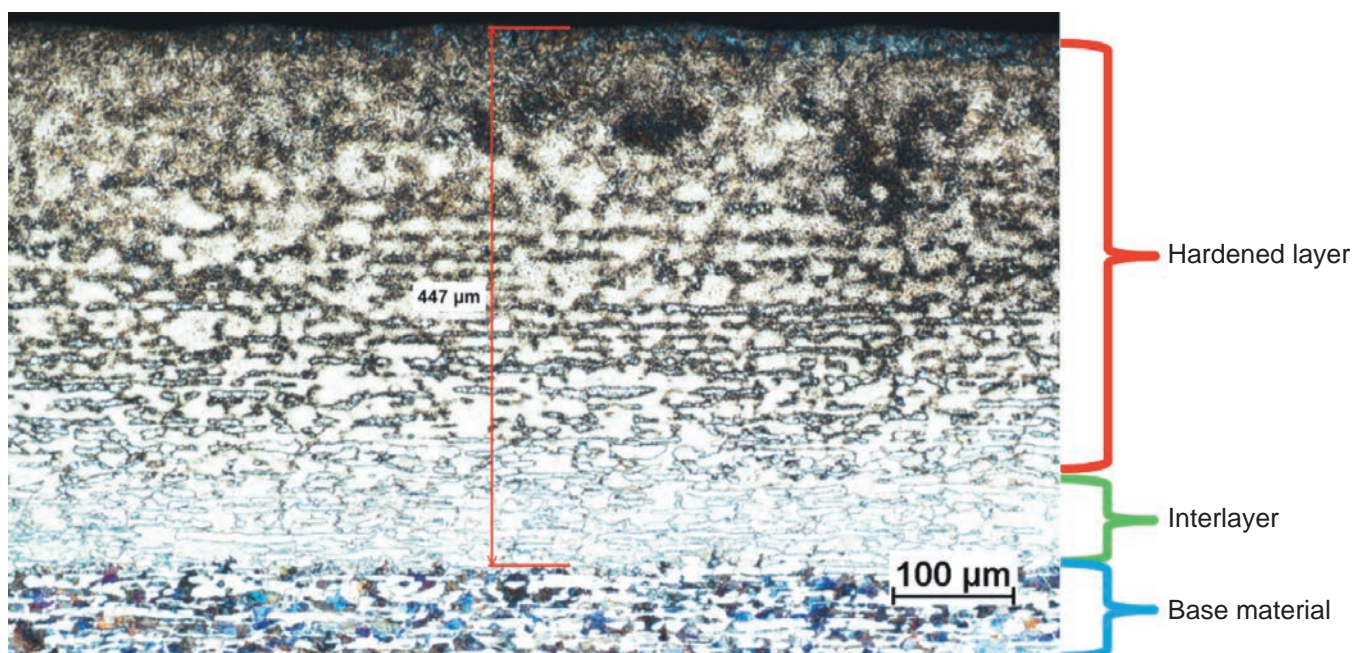


Fig. 5. Cross-section of the specimen subjected to hardening using a beam current of 29 mA

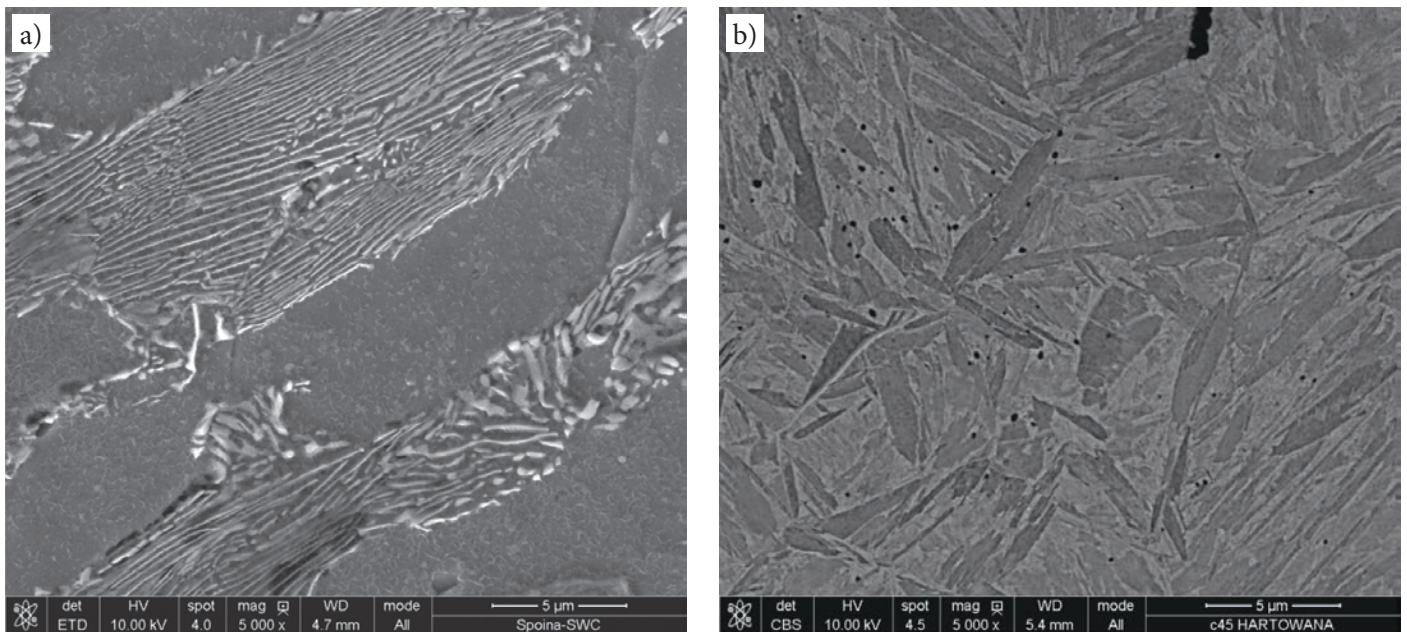


Fig. 6. View of a) ferritic-pearlitic microstructure of the base material and b) martensitic microstructure of the hardened subsurface layer

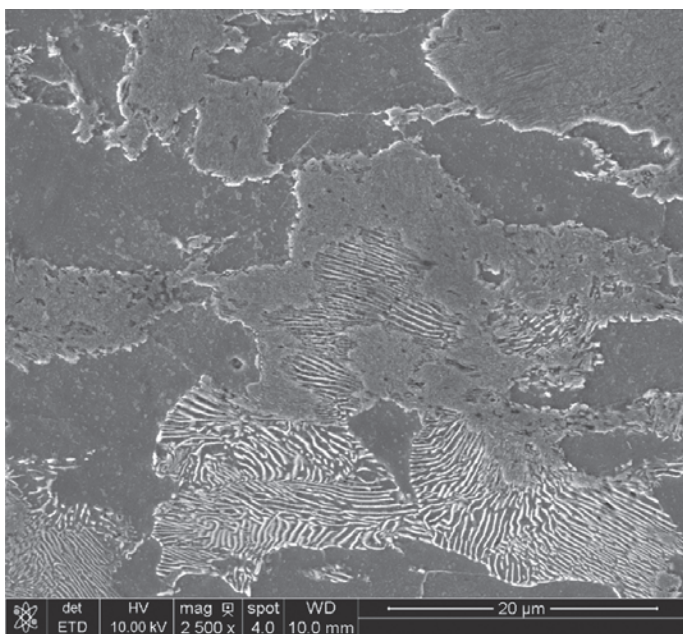


Fig. 7. Martensitic-pearlitic-ferritic structure of the inter-layer

of depth measured from the surface and the width of the hardened layer (in relation to selected specimens and an electron beam current of 25 mA, 27 mA and 29 mA respectively). The specimens hardened using a beam current of 27 mA and 29 mA were characterised by the most uniform distribution of hardness in the hardened zone. The remaining specimens were characterised by the non-uniform distribution of hardness. The hardened area was characterised by a width of approximately 10 mm wide and the HAZ depth from the surface restricted within the range of 0.3 to 0.45 mm; the effective hardening depth was restricted within the range of 0.15 mm to 0.3 mm.

Table 1. Maximum hardness and HAZ depth in relation to electron beam power

| No. | Beam current (mA) | Beam power (W) | HAZ depth (mm) | Maximum hardness (HV0.1) | Average hardness at a depth of 0.15 mm (HV0.1) |
|-----|-------------------|----------------|----------------|--------------------------|--|
| 1 | 29 | 1740 | 0.447 | 1039 | 810 |
| 2 | 28 | 1680 | 0.353 | 944 | 787 |
| 3 | 27 | 1620 | 0.326 | 960 | 813 |
| 4 | 26 | 1560 | 0.326 | 1035 | 769 |
| 5 | 25 | 1500 | 0.303 | 1102 | 701 |

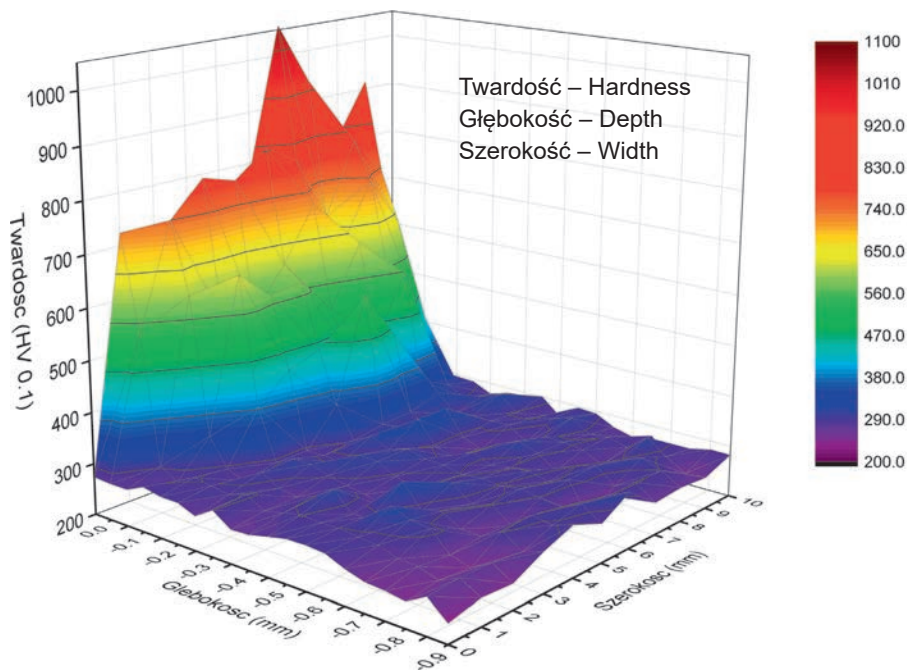


Fig. 8. Distribution of hardness in the specimen hardened using an electron beam current of 25 mA

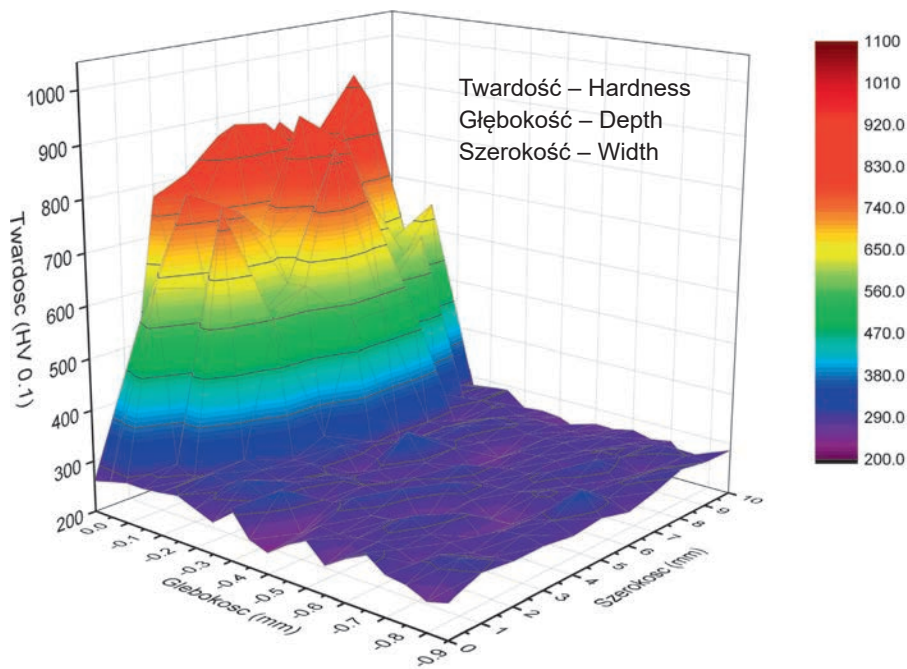


Fig. 9. Distribution of hardness in the specimen hardened using an electron beam current of 27 mA

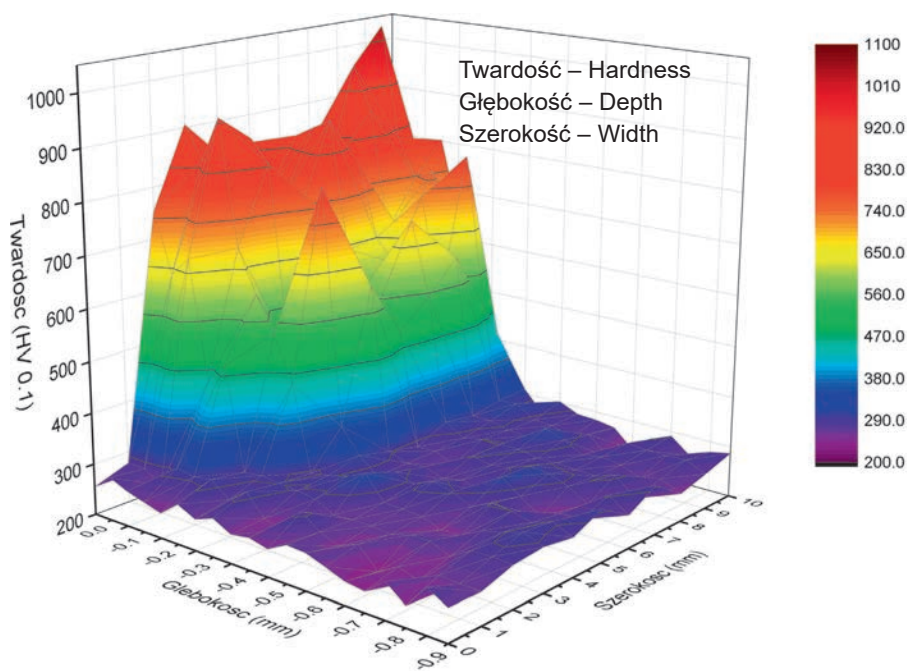


Fig. 10. Distribution of hardness in the specimen hardened using an electron beam current of 29 mA

Summary

The tests discussed in the article revealed that electron beam hardening (EBH) could be used successfully in relation to steel grade C45. In comparison with values presented in examples contained in reference publications, the maximum hardness obtained in the tests exceeded that obtainable using the remaining surface hardening methods. The surface of the test specimens did not undergo partial melting, but only the desirable martensitic transformation. The microstructure of the hardened layer was composed of martensite, whereas that of the interlayer constituted the mixture of martensite, pearlite and ferrite. Both the HAZ depth and the effective hardening depth increased along with increasing electron beam current. The highest hardness of 1102 HV_{0.1} was obtained in the specimen hardened using the lowest current (25 mA). As mentioned before, the specimens hardened using an electron beam power of 27 mA and 29 mA were characterised by the most uniform distribution of hardness in the hardened area and, consequently, the highest average hardness values amounting to 813 HV_{0.1} and 810 HV_{0.1} respectively. The distribution of hardness in the remaining specimens was non-uniform. Because of the possible precise deflection of the beam and very good properties of the hardened layers, the electron beam hardening technology can be used successfully in providing elements characterised by complicated geometry with layers exposed to intense abrasion.

Acknowledgements

The tests discussed in the article, performed at Łukasiewicz Research network – Institute of Welding, were financed by the Ministry of Science and Higher Education within research work no. Cd-2 (ST-12/21) entitled *Tests of Thermal Surface Hardening with Respect to Fatigue Service Life*.

References

- [1] Pilarczyk J., Węglowski M.S.: Spawanie wiązką elektronów Electron beam welding. *Welding Technology Review*, 2015, vol. 87, no. 10, pp. 124–129.
- [2] Śliwiński P., Węglowski M.S., Kwieciński K., Wieczorek A.: Hartowanie powierzchniowe wiązką elektronów – przegląd zagadnienia Electron beam surface hardening. *Biuletyn Instytutu Spawalnictwa*, 2022, vol. 66, no. 1, pp. 9–18.
- [3] DVS Technical Codes on Electron Beam Welding. English Edition. 2013. Vol. 8. ISBN 978-3-87155-244-1.
- [4] Schulze K.-R.: *Electron Beam Technologies*. Wissen kompakt. 2012, DVS Media, ISBN 3-87155-227-5.
- [5] Valkov S., Ormanova M., Petrov P.: *Electron-Beam Surface Treatment of Metals and Alloys: Techniques and Trends*. *Metals*, 2020, no. 10, 1219.
- [6] Ribton C.: Intelligent power supplies for electron beam welding at 300 kV and 150 kW. *IEE Colloquium on Power Electronics for Demanding Applications* (Ref. no. 1999/059), 1999, pp. 4/1–4/7.
- [7] Pawłowski B.: *Obróbka cieplna i cieplno-chemiczna stali*. Praca zbiorowa pod redakcją J. Pacyny: *Metaloznawstwo*. Wybrane zagadnienia. Uczelniane Wydawnictwo Naukowo-Dydaktyczne AGH, 2005, pp. 175–202.
- [8] Jankowski T., Głowacka M.: *Hartowanie i odpuszczanie stali węglowych*. Praca zbiorowa pod redakcją J. Hucińskiej: *Metaloznawstwo*. Materiały do ćwiczeń laboratoryjnych. Wydawnictwo Politechniki Gdańskiej, 1995, pp. 107–129
- [9] Dossett J., Totten G.E.: *Steel Heat Treating Fundamentals and Processes*. Introduction to Surface Hardening of Steels. *ASM Handbook*, Vol. 4A. Revised by Michael J. Schneider, The Timken Company, and Madhu S. Chatterjee, 2013.

- [10] Łomozik M.: Mikrostruktury złączy spawanych stali konstrukcyjnych oraz spawalnicze wykresy przemian austenitu CTPc-S. Monograph (unpublished). Sieć Badawcza Łukasiewicz – Instytut Spawalnictwa, Gliwice 2022.
- [11] Vieira E.R., Biehl L.V., Medeiros J.L.B. et al.: Evaluation of the characteristics of an AISI 1045 steel quenched in different concentration of polymer solutions of polyvinylpyrrolidone. *Scientific Reports*, 2021, vol. 11, 1313.
- [12] Magnabosco I., Ferro P., Tizani A., Bonollo F.: Induction heat treatment of a ISO C45 steel bar: Experimental and numerical analysis, *Computational Materials Science*, 2006, vol. 35, no. 2.
- [13] Bouquet J., Van Camp D., Vanhove H., Clijsters S., Amirahmad M., Lauwers B.: Development of a Flexible Laser Hardening & Machining Center and Proof of Concept on C-45 Steel. *Physics Procedia*, 2014, vol. 56, pp. 1083–1093. <https://doi.org/10.1016/j.phpro.2014.08.021>.
- [14] Teirumnieks N.: Laser hardening of steel C45. 21. Starptautiskā studentu zinātniski praktiskā konference Cilvēks.Vide.Tehnoloģijas. 2017, pp. 204–209. <http://dx.doi.org/10.17770/het2017.21.3565>.
- [15] Song R.G., Zhang K., Chen G.N.: Electron beam surface treatment. Part I: surface hardening of AISI D3 tool steel. *Vacuum*, 2003, vol. 69, no. 4, pp. 513–516.
- [16] Katsuyuki M. Shiroh, Takayuki H., Masahiko K.: Electron beam hardening. *Int. J. of Materials and Product Technology*, 1990, vol. 5, no. 3.
- [17] Storch W., Mühl F., Schulze K.R.: Electron beam hardening for the regeneration of turbine blades. *Welding International*, 1988, vol. 2, no. 12, pp. 1127–1130.
- [18] Matlák J., Dlouhý I.: Properties of Electron Beam Hardened Layers made by Different Beam Deflection. *Manufacturing Technology*, 2018, Vol. 18, pp. 279–284.
- [19] Petrov P. Optimization of carbon steel electron-beam hardening *J. Phys.: Conf. Ser.* 223 012029. 2010.
- [20] Friedel K.P., Felba J., Pobol I., Wymysłowski A.: A systematic method for optimizing the electron beam hardening process. *Vacuum*, 1996, vol. 47, no. 11, pp. 1317-1324.